Everolimus improves the efficacy of dasatinib in the treatment of PDGFRA-driven glioma

Zachary Miklja[1^], Viveka Nand Yadav[1^], Rodrigo Cartaxo[1], Ruby Siada[1], Brendan Mullan[1], Stefanie Stallard[1], Alyssa Paul[1], Amy K. Bruzek[2], Kyle Wierzbicki[1], Tao Yang[4], Taylor Garcia[1], Ian Wolfe[1], Hemant Parmar[6], Marcia Leonard[1], Patricia L. Robertson[1], Hugh Garton[2], Sriram Venneti[3], Chandan Kumar-Sinha[3,5], Arul Chinnaiyan[3,5,8,9], Rajen Mody[1], Manjunath P. Pai[11], Timothy N. Phoenix[12], Bernard L. Marini[11], Carl Koschmann[1*]

Affiliations: [1]University of Michigan Medical School Department of Pediatrics, [2]Department of Neurosurgery, [3]Department of Pathology, [4]Department of Neurology, [5]Department of Urology, [6]Department of Radiology, [7]Michigan Center for Translational Pathology, [8]Howard Hughes Medical Institute, [9]Rogel Cancer Center, [10]Clinical Pharmacy, [11]College of Pharmacy, Michigan Medicine, Ann Arbor, MI 48109, USA. [12]University of Cincinnati College of Pharmacy, Cincinnati, OH 45627, USA.

Correspondence:

Carl Koschmann, M.D.
Department of Pediatrics,
Division of Pediatric Hematology/Oncology
University of Michigan Medical School
3520D MSRB 1, 1150 W Medical Center Dr.
Ann Arbor MI, 48109
Phone: +1-734-936-9814
Fax: +1-734-763-2543
Email: ckoschma@med.umich.edu

Conflict of Interest: A.M.C. is on the Scientific Advisory Board at Tempus.

"*corresponding author"

"^denotes equal contribution"

Abstract:

Background: Pediatric and adult high-grade glioma (HGG) frequently harbor *PDGFRA* alterations. Treatment of PDGFRA-driven HGG with targeted agents, such as the tyrosine kinase inhibitor dasatinib, has failed in the clinic. We hypothesized that co-treatment with everolimus may improve the efficacy of dasatinib in PDGFRA-driven glioma through combinatorial synergism and increased tumor accumulation of dasatinib.

Methods: Dose response, synergism studies, P-gp inhibition and pharmacokinetic studies were performed on *in vitro* and *in vivo* human and mouse models of HGG. *De novo* tumors were generated in mice using intra-uterine electroporation (IUE) by injecting PB plasmids of *TP53* mutation, *PDGFRA* mutation and H3K27M mutation (PPK) in the lateral vertical of mice embryos. Two children with recurrent PDGFRA-driven HGG were treated with dasatinib and everolimus with correlate CSF analysis.

Results: Dasatinib effectively inhibited the proliferation of mouse and human primary HGG cells with a dose-dependent reduction of PDGFRA and pPDGFRA. Dasatinib exhibited synergy with everolimus in the treatment of HGG cells at low nanomolar concentrations of both agents. Prolonged exposure to everolimus significantly improved the CNS retention of dasatinib and extended survival of PPK tumor bearing mice. Two children with recurrent PDGFRA-driven HGG treated with dasatinib and everolimus survived six months and nine months after progression. A paired CSF sample from the

patient with *PDGFRA*-amplified HGG showed 50% increase in CSF dasatinib levels after the addition of everolimus.

Conclusion: Efficacy of dasatinib treatment of PDGFRA-driven HGG is improved with everolimus and suggests a promising route for improving targeted therapy for this patient population.

Trial Registration: ClinicalTrials.gov NCT03352427

Funding: The authors thank the patients and their families for participation in this study. CK is supported by NIH/NINDS K08-NS099427-01, the University of Michigan Chad Carr Pediatric Brain Tumor Center, the Chad Tough Foundation, Hyundai Hope on Wheels and Catching up with Jack. The PEDS-MIONCOSEQ study was supported by grant 1UM1HG006508 from the National Institutes of Health Clinical Sequencing Exploratory Research Award (PI: Arul Chinnaiyan).

INTRODUCTION

High-grade gliomas (HGGs) are common and aggressive pediatric and adult brain tumors. Median overall survival (OS) of adult patients diagnosed with glioblastoma (GBM), grade IV glioma, is 12.6 months (1), and median OS for pediatric HGG is 14.1 months (2). Established therapies for adult and pediatric HGG are not currently targeted to the unique molecular attributes of each tumor, and patients frequently consider experimental therapies after up-front radiation and at recurrence.

One of the most frequently altered genes in HGG is platelet-derived growth factor receptor alpha (*PDGFRA)*. PDGFRA is one of two PDGF receptor subunits, and it interacts with at least four PDGF ligands (3). It has been shown that PDGF activation induces multiple cellular activities including cell proliferation, transformation, migration, and survival (3). *PDGFRA* is mutated or amplified in 12% of adult GBM and 21% of pediatric HGG (4,5). Within childhood HGG, *PDGFRA* mutation is correlated with older age (10-30 years), while amplification is seen more commonly in younger patients (5-10 years) (5). *PDGFRA* alterations are drivers of aggressive glioma behavior and are associated with worse prognoses in pediatric non-brainstem HGG and adult anaplastic astrocytoma (WHO grade III glioma) (5,6).

Pre-clinically, there are multiple effective agents targeting PDGFRA in glioma, including the tyrosine kinase inhibitor (TKI) dasatinib (5,7). Unfortunately, monotherapy with dasatinib has failed to improve outcomes in adult HGG, even when gliomas were selected for by PDGFRA overexpression by IHC (8). The failure of dasatinib may be related to its use as a single agent. Recent data in other solid tumors has demonstrated

synergism between TKIs and the mTOR inhibitor everolimus, including the clinical success of lenvatinib and everolimus for renal cell carcinoma (9). Osteosarcoma pre-clinical models treated with sorafenib overcame resultant upregulation of mTORC1 (mTOR complex 1) through co-treatment with everolimus (10).

Additionally, treatment with dasatinib for CNS tumors may be limited by CNS penetration. Based on its intrinsic qualities (i.e. lipophilicity, size, and protein binding), dasatinib is a promising agent for CNS penetration (11). While the ability of dasatinib to penetrate the blood-brain barrier (BBB) is promising, its retention is limited by CSF efflux proteins P-glycoprotein (P-gp) and breast cancer resistance protein (BCRP) (12). Recent work has demonstrated that co-administration of TKIs with agents that inhibit P-gp and Bcrp1 can improve the brain retention of the TKI (12-14). Everolimus has been shown to improve the CNS retention of the TKI vandetanib (13).

To date, co-administration of dasatinib and everolimus has never been tested in CNS tumor models or administered to human patients with *PDGFRA*-driven gliomas. In this study, we assessed whether co-treatment of dasatinib with everolimus could improve the efficacy and CNS retention of dasatinib in *PDGFRA*-driven gliomas in both pre-clinical models and human patients. We found that everolimus acts synergistically with dasatinib in *PDGFRA*-driven glioma. We also found that sustained everolimus administration results in significant increases in tumor concentrations of dasatinib in a genetically-engineered HGGanimal model. Preliminary data from two patients treated establishes promising feasibility. Our findings represent a novel route for enhancing the efficacy of TKI precision therapy for pediatric and adult HGG.

RESULTS:

Generation of TP53, PDGFRA and H3K27M mutant (PPK) glioma primary cell cultures and in vitro *treatment with dasatinib*

In order to study the utility of dasatinib in PDGFRA-driven HGG, we developed an intra-uterine electroporation (IUE) mouse model (Fig. 1A). We induced glioma in mice by injecting plasmids encoding: [1] PBase; [2] PB-CAG-DNp53-Ires-Luciferase ("TP53"); [3] PB-CAG-PdgfraD824V-Ires-eGFP ("PDGFRA D842V"); and [4] PB-CAG-H3.3 K27M-Ires-eGFP ("H3K27M") into the lateral ventricles (forebrain) of embryos in CD1 mice at E13.5 days. Transfection efficiency and tumor growth were monitored by *in vivo* imaging of luminescence (Fig. 1A). With the injection of PPK plasmids, mice developed high-grade, invasive glial tumors (Supplementary Figure S1A) with a high penetrance (>90%) and a median survival of 77 days. IHC analysis showed tumor-specific expression of H3.3 K27M, elevated PDGFRA and reduced expression of H3.3K27me3 (Supplementary Figure S1A). Multiple TP53, PDGFRA and H3K27M (PPK) mutant glioma primary neurosphere cultures were generated from dissociation of intra-cranial tumor tissue from these mice (Fig. 1A).

Previous studies have demonstrated that tumor cells driven by *PDGFRA* D842V mutation may be relatively PDGF α and β ligand-insensitive (as compared to *PDGFRA* amplification) (7). However, we found a dose-dependent increase in proliferation when cells were supplemented with ligands PDGF α and β (Fig. 1B). Supplementation with PDGF α and β ligand also led to increase in activated [p-PDGFRα (y-849)] and total PDGFRα (Fig. 1C and Supplementary Figure S1B).

PPK cells demonstrated sensitivity to monotherapy with dasatinib *in vitro*, with an IC_{50} of 100 nM (Fig. 1D) and dose dependent reduction in p-PDGFRα (y-849) and PDGFRα total protein expression (Fig. 1E). We analyzed publicly available human glioma cell culture dasatinib treatment data (n=12) from the Genomics of Drug Sensitivity in Cancer (GDSC) (15). Glioma cell cultures demonstrated promising sensitivity to dasatinib in general (Supplementary Figure S2A). Dasatinib demonstrated improved efficacy in glioma cell cultures with *PDGFR* alterations (Fig. 1F). Additionally, we performed dasatinib treatment on three pediatric glioma lines. UMPED05 and UMPED58, thalamic and brainstem HGG primary cell cultures with *PDGFRA* amplification, demonstrated strong sensitivity to dasatinib (Fig. 1F). KNS42, a pediatric HGG line without *PDGFRA* alteration, demonstrated an IC_{50} of 20 uM, consistent with our previous results (5). UMPED58 glioma cell culture demonstrated increased proliferation when grown with ligand PDGF α and β ($P \leq 0.0001$) (Supplementary Figure S2B-C). Collectively, this data demonstrated that dasatinib selectively and effectively inhibits proliferation in mouse and human HGG with various *PDGFR* alterations.

Addition of everolimus provides synergism

Previous work has established that TKIs may have improved efficacy in combination with the mTOR inhibitor everolimus (9,10). We assessed whether everolimus provided synergistic benefit in the treatment of our glioma model. PPK cells were treated with escalating combinations of dasatinib and everolimus for synergism analysis (Fig. 2A). At all doses of everolimus, dasatinib demonstrated dose-dependent reduction in PPK neurosphere viability (Fig. 2A). Interestingly, everolimus contributed to

reduced proliferation at even the lowest dose (1 nM), but displayed little dose-dependent effect at higher doses (Fig. 2A). *In vitro* monitoring demonstrated neurosphere disruption with both agents as monotherapy, although more significantly with dasatinib (Fig. 2B and Supplementary Figure S3A). Using the Chou-Talalay median-effect method for drug combination analysis, everolimus and dasatinib demonstrated synergistic effect at nearly all dose combinations, including single nanomolar doses of both agents (Fig. 2C).

Everolimus provides P-gp blockade at higher dose

Previous work has established that dasatinib is a substrate for efflux proteins P-gp and BCRP (16-19). As P-gp is likely the predominant substrate affecting CNS efflux (14), we focused our attention on P-gp. To assess the P-gp inhibitory effects of everolimus, we performed an *in vitro* P-gp inhibition assay. Everolimus fully blocked P-gp activity at 1 μM at four hours (Fig. 2D and Supplementary Figure S3B). Lower doses of everolimus (10 nM) were not significantly different from non-treated cells (Fig. 2D). The effect at 1 μM concentrations was similar to slightly lower than previous levels of everolimus (3-5 μM) necessary for P-gp inhibition in Madin-Darby canine kidney (MDCK) cells over-expressing multi-drug resistance genes (P-gp and BCRP)(20).

Pharmacokinetic (PK) analysis of dasatinib and everolimus CNS retention

We then proceeded to test the effect of everolimus on CNS concentrations of dasatinib in non-tumor bearing mice. Mice were treated with dasatinib (25 mg/kg tail vein injection) with or without a single dose of everolimus (10 mg/kg oral gavage administration) two hours prior. Mice were sacrificed at one, two, four, and seven-hour

time points (n=3 each) for collection of serum, brainstem and cortex (Supplementary Figure S4A). We did separate analysis of brain and brainstem PK because previous literature and clinical experience suggest that the blood-brain barrier (BBB) is more restrictive in the brainstem (21). No statistically significant differences were found for dasatinib concentrations between the two conditions (dasatinib alone and dasatinib with everolimus) within the plasma, cortex, and brainstem (Supplementary Figure S4B-F). Average plasma concentrations of dasatinib were higher in co-treated mice, although this was not statistically significant. Pharmacokinetic analysis of everolimus monotherapy in non-tumor bearing mice demonstrated an increase in everolimus concentrations (ng/g) within mouse brain tissue over time (Supplementary Figure S5A-B).

Sustained exposure of everolimus improves dasatinib tumor delivery and increases survival of mice bearing PPK tumor

We then proceeded to our IUE murine model of HGG to assess whether intra-tumor concentration of dasatinib would be impacted by co-treatment with everolimus (Fig. 3A). We confirmed up-regulation of total PDGFRA and downstream activation of p-AKT within the tumors of our PPK mouse tumor model (Fig. 3B). We performed treatment studies in mice with large cortical PPK tumors that met enrollment luminescence criteria (average 32 dpi). As seen in our non-tumor bearing mice, single dose treatment of everolimus did not influence the tumor concentration of dasatinib (Fig. 3C). However, with the addition of a second dose of everolimus 24 hours prior to dasatinib, tumor concentrations of dasatinib were increased eight fold (Fig. 3C). Importantly, the average tumor concentration of dasatinib was significantly higher than

in vitro IC_{50} calculations for PPK and human PDGFRA-driven cells. In additional tumor bearing mice treated with two doses of everolimus prior to dasatinib treatment immediately before sacrificing demonstrated reduced expression of, P-gp, pAKT and PDGFR by IHC. (Fig. 3D and Supplementary Figure S6A-C).

To assess the effect of sustained co-treatment on survival, IUE PPK mice were treated in four separate conditions: vehicle, daily treatment with dasatinib alone, daily treatment with everolimus alone, and daily co-administration with dasatinib and everolimus, for one week. Co-treatment resulted in statistically significant improvements in survival (Fig. 3E). At 76 days post IUE injection, the dasatinib and everolimus treated mice demonstrated reduced average luminescent tumor signals than control mice, although this was not statistically significant (Fig. 3F).

Treatment of children with relapsed PDGFRA-driven glioma with dasatinib and everolimus

Based on this promising pre-clinical data, we moved forward with pursuit of clinical treatment with daily dasatinib and everolimus for PDGFRA-driven glioma in human patients. Patients with recurrent HGG have no proven therapies and an expected overall survival of four to six months (22,23). In order to determine the impact of everolimus on dasatinib CNS retention, we developed a protocol and received IRB approval to treat children and adults with confirmed PDGFR-altered glioma with paired CSF/plasma samples after one week of dasatinib mono-therapy and then after 2 cycles of dual therapy (Fig. 4A).

We treated two children with recurrent HGG on this regimen. Our first patient (UMPED44) was a seven-year-old female with a history of recurrent thalamic HGG.

From the patient's partial resection at diagnosis, the tumor was found to have a somatic point mutation in *TP53* (and copy neutral LOH), amplification and over-expression of *PDGFRA* and *MET*, and homozygous deletion of *CDKN2A* (Fig. 4B-C). Additionally, CSF tDNA at baseline demonstrated an elevated *PDGFRA* copy number (Fig. 4D). The patient underwent treatment with everolimus and dasatinib for three months before showing further progression, and survived six months from initial progression (Fig. 4E). This patient tolerated dual therapy well with rash attributed to dasatinib but not requiring dose modification. Treatment resulted in a 50% increase in CSF dasatinib level with combined treatment with everolimus (Supplementary Figure S7).

Our second patient (UMPED52) was a four-year-old female with a recurrent DIPG. Sequencing at progression demonstrated no significant copy number alterations (Supplementary Figure S8A) and somatic point mutations of *PDGFRA* (D824V), *ACVR2B* and *DCC* (Supplementary Figure S8B). Cerebrospinal fluid tumor DNA (CSF tDNA) at baseline demonstrated *PDGFRA* D824V variant allele fraction of 34% (Supplementary Figure S8C). The patient underwent treatment for four cycles with clinical and radiographic stability followed by clinical and radiographic progression at five months and survival nine months from first progression. This patient tolerated therapy with no side effects or adverse events (Supplementary Figure S8D). When treated with dasatinib alone, UMPED52 plasma dasatinib concentration was 26.4 ng/mL, and when treated with both dasatinib and everolimus, plasma concentration of dasatinib was 165.0 ng/mL (Supplementary Figure S7A). Unfortunately, due to technical difficulties, CSF samples did not result in interpretable dasatinib PK results.

P-gp expression in human HGG RNA-seq datasets

As P-gp is expressed both in brain and tumor cells, and overall expression at protein level was reduced in our mouse HGG models after sustained treatment with everolimus, we were interested to explore if P-gp expression correlated with clinical or genomic features in human datasets. We analyzed RNA-seq data from pediatric HGGs within PedcBioPortal, [Pediatric HGG ICR London dataset, n = 1067(2)] and found that P-gp expression was highest in: (a) pediatric hemispheric HGG, (b) tumors with wild type *H3F3A* (gain of function mutations are found in half of pediatric HGG), and (c) young adult age patients (age 10-15) (Fig. 5A). Importantly, P-gp expression was higher in pediatric HGG with *PDGFRA* alterations (Fig. 5A, n= 147). In analysis of adult HGGs (cBioPortal, TCGA dataset, n = 585) (24), no clinical parameters showed correlation with P-gp expression, including PDGFRA status, MGMT status and age at diagnosis (Supplementary Figure S9A).

DISCUSSION:

Our study illustrates that everolimus improves the efficacy of dasatinib in the treatment of PDGFRA-driven glioma. While response attribution is difficult for two consecutive cases, our early clinical experience with this combination demonstrated excellent tolerance of the regimen and overall survival from progression that compares favorably to historical controls (22,23). To our knowledge, the use of everolimus co-treatment with dasatinib had not previously been tested in glioma tumor models or human patients. More broadly, our results demonstrate that TKI treatment targeted to alterations in HGG may have renewed clinical relevance when combined with mTOR inhibitors.

Importantly, our murine IUE tumor model experiments demonstrate that everolimus and dasatinib display synergistic activity in the treatment of PDGFR-driven glioma cells. This may be due to the presence of dual inhibition within the PDGFRA/PI3K/AKT/mTOR cell proliferation pathway: dasatinib inhibits PDGFRA and everolimus inhibits mTOR further downstream (5,25) (Fig. 5B). Attribution to tumor cell toxicity from improved intra-cellular dasatinib concentration vs. direct mTOR inhibition is difficult to fully distinguish. However, we found no *in vitro* P-gp inhibition with everolimus treatment at low dose (10 nM), while our treatment studies show significant contribution of everolimus to reduced tumor cell viability at 1 nM,

In our *in vivo* model, the administration of everolimus increases tumor concentrations of dasatinib above therapeutic (IC_{50}) levels, and that this increase required sustained (>24 hours) everolimus exposure. This requirement may be related to the time required for protein-level changes (i.e. reduced P-gp expression and/or activity) to occur. Interestingly, dasatinib concentrations were raised more prominently in the CNS tumor samples than the brain itself. This may be due to the disruption of the BBB in high-grade tumors, allowing for greater dasatinib influx (26). Indeed, our murine tumor demonstrated high-grade features that may influence BBB integrity, including necrosis and vascular proliferation (Fig S1A).

A concern with P-gp inhibition strategies that remains in our study is whether the inhibitor itself can get into the CNS at high enough concentrations to achieve P-gp inhibition (27). Our data showed a concentration of everolimus required for P-gp inhibition that was achievable in the plasma (~10 uM) and brain (~1 uM) of our mouse models, but may be more difficult to achieve in human brains with current clinical trough goals (5-15 ng/mL, or ~5-15 nM). Interestingly, early adult phase 1 studies of

everolimus studied weekly higher dosing of everolimus (up to 70 mg), which resulted in mean peak levels of everolimus of 175 ng/ml (190 nM), and tolerability similar or better than daily 10 mg dosing (28). Future studies may clarify whether everolimus inhibits P-gp at this dosing or whether higher dosing of everolimus should be re-considered. P-gp also promotes efflux on the luminal side of blood vessels (Fig. 5B), and so future clinical efforts to achieve Pg-P inhibition may be based on plasma (rather than brain parenchyma) concentrations of everolimus. At a minimum, based on our *in vitro* models, everolimus would contribute to synergistic cytotoxicity of PDGFR-driven HGG in clinically relevant (~low nM) concentrations of everolimus and dasatinib.

While everolimus may help prevent efflux of dasatinib out of brain parenchyma and tumor cells, the efficacy of dasatinib will ultimately rely on the cells' sensitivity to it, which may be variable based on the type of *PDGFRA* alteration expressed by the cells. The *PDGFRA* alteration in each glioma can strongly contribute to the sensitivity to dasatinib (7). Our PPK cells carry the recurrent *PDGFRA* D842V mutation (as did patient UMPED52) and displayed sensitivity (IC_{50} 100 nM) to dasatinib. Previous studies have shown mixed sensitivity of the D842V mutant to dasatinib, including reduced sensitivity to dasatinib in $PDGFRA^{D842V}$-mutant normal human astrocytes (NHAs) (7). However, nanomolar reduction in D842V-mutant kinase activity has been demonstrated in gastro-intestinal stromal tumor (GIST) tumors (29). Importantly, our IUE-based PPK cells retain endogenous, wild-type *PDGFRA*, which may contribute to tumor proliferation and dasatinib sensitivity. Future studies will continue to clarify the responsiveness of various *PDGFRA* alterations to dasatinib sensitivity, but our data demonstrates promise of this dual therapy in both *PDGFRA*-mutant and amplified gliomas.

While still preliminary, our early clinical experiment is promising. Our two patients experienced modest progression-free survival (PFS) (three months and five months). However, their OS from progression (six months and nine months) was encouraging in comparison to historical controls for relapsed pediatric HGG (four to six months) (22,23). While we did find an increase in CSF dasatinib levels after everolimus co-administration in UMPED44, the overall CSF dasatinib concentration (~2 nM) still remained near or below the IC_{50} of most human PDGFRA-drive glioma cell cultures. We are using CSF as the best proxy for dasatinib concentrations within the tumor, and it may not be an accurate reflection of tumor concentration. Indeed, in our murine model, cortex concentrations of dasatinib were consistently lower than tumor concentrations. Future patient data will help clarify the CSF retention of dasatinib, and future clinical studies may consider further dose escalation of dasatinib.

Thus far, targeted treatments for PDGFRA-driven HGG have failed to improve outcomes in both adult and pediatric patients. This shortcoming has exposed the need for new precision medicine approaches for these patient population. Our study confirms that dasatinib effectively inhibits PDGFRA, and the sustained co-administration of dasatinib and everolimus allows for additional synergistic efficacy and the potential for improved CNS penetration. The combination of dasatinib and everolimus represents a new avenue for adult and pediatric HGG treatment, and the co-administration of these drugs re-opens the possibility of dasatinib being an effective therapy for PDGFRA-driven glioma.

METHODS:

Murine model of high-grade glioma using intra-uterine electroporation.

In utero electroporation (IUE) was performed using sterile technique on isoflurane/oxygen-anesthetized pregnant CD1 females at embryonic stage E 13.5 (cortex), using established methodology (30). All tumors for this study were generated by injecting plasmids either in the lateral ventricle (forebrain) or in the fourth ventricle (hindbrain). In this study we injected the following four plasmids together: [1] PBase, [2] PB-CAG-DNp53-Ires-Luciferase (dominant negative TP53 or TP53 hereafter), [3] PB-CAG-PdgfraD824V-Ires-eGFP (PDGFRA D842V), and [4] PB-CAG-H3.3 K27M-Ires-eGFP (H3K27M), referred to as “PPK” model.

All animal studies were conducted according to the guidelines approved by the University Committee on Use and Care of Animals (UCUCA) at the University of Michigan. Following anesthesia induction, Carprofen was administered subcutaneously for additional analgesia. Uterine horns were exposed through a 1 cm incision, and individual embryos were digitally manipulated into the correct orientation for intraventricular injection. A pulled capillary needle was loaded with endotoxin-free DNA and Fast Green dye (0.05%, Sigma-Aldrich) for visualization, and a microinjector was used to inject either the lateral or fourth ventricles with the DNA-dye mixture. 3-4 plasmids were injected simultaneously, each at a final concentration of 1 μg/μl and 1-2 μl of total solution was injected per embryo. DNA was then electroporated into cortical neural progenitors using 5 mm tweezertrodes (BTX), applying 5 square pulses at 35 V, 50 ms each with 950 ms intervals. The embryos were then returned into the abdominal cavity, the muscle and skin were sutured and the animal was monitored until fully recovered from the procedure.

After delivery, the efficacy of plasmids uptake was monitored by bioluminescence with the IVIS Spectrum (tumors express luciferase). Pups that did not

display bioluminescence were euthanized, which occurred in about 5 to 10 percent of the pups. After three weeks, juveniles were weaned and separated by gender. The mice with positive signal were monitored for tumors every day by observation and biweekly bioluminescence imaging on an IVIS Spectrum imaging system until the signs of intracranial tumor burden ensued.

Generation of IUE primary HGG cell cultures

Mouse HGG primary cell cultures were generated by harvesting IUE tumors at the time of euthanasia. Tumors were located by green fluorescent protein (GFP) expression under an epi-fluorescent microscope (Olympus CKX41) at the time of resection. The tumor mass was gently homogenized and dissociated with non-enzymatic cell dissociation buffer (Gibco). Cell suspension was filtered through a 70 μm cell strainer, centrifuged at 300 x g for 4 min, and re-suspended into 7 ml of Neurobasal-A Medium (1x) Base media (Invitrogen, 500 mL). Each base stock of media was supplemented with 10 mL B27 with vitamin A, 5 mL N2, 5mL Sodium Pyruvate (1 mM), 5 mL non-essential amino acids (100 uM), 7.5 mL L-glutamine (2 mM), 1mL Normocin, 5 mL Antibiotic-Antimycotic, and 1μL EGF (20ng/mL) per 1 mL media every three days.

In vitro *treatment and synergism calculations*

IUE-generated PDGFRA-driven HGG primary cell culture (PPK) were cultured in conditions as described above. Cell viability *in vitro* was monitored either by XTT Cell Proliferation Assay kit (Cayman Chemical) utilizing the included protocol, or bioluminescence readings collected using the Synergy HTX Multi-Mode micro plate-reader (BioTek). Additionally, cell proliferation was monitored via IncuCyte Zoom live-cell analysis. Through use of the IncuCyte Zoom live imager, the growth of 3,000 PPK

primary cells plated in 96 wells was monitored by units of average green fluorescent intensity (GCU x um2). PPK primary cell culture was grown with 200 µL of media and 1 µL of PDGF-AA and PDGF-BB at working concentration of 10 ng/mL in each 96 well (Shenandoah Biotechnology, Inc.). All *in vitro* treatments were completed with research-grade dasatinib and everolimus (Selleck). UMPED58 is a primary human cell line generated from a 7-year-old male with DIPG at autopsy. At diagnosis, tumor was sequenced and found to carry *H3F3A K27M*, *ATRX pQ119**, and *PDGFRA*, *KIT* and *KDR* amplifications. UMPED05 is a primary cell line generated from a 2-year-old female with thalamic HGG at autopsy with *PDGFRA* amplification, as previously described by Koschmann et al. (2016) (5). Both UMPED58 and UMPED05 were grown in 10 mL L-glutamine (200mM), 5 mL 100x penicillin streptomycin (pen strep), 10% fetal bovine serum. All synergism calculations were performed by the Chou-Talalay method for drug combination based on the median-effect equation (31).

Murine IUE HGG treatment studies

Mice harboring IUE-generated PPK HGG tumors were treated with everolimus and/or dasatinib. Mice were treated when tumors reached logarithmic growth phase (minimum 2 x 10^5 photons/sec via bioluminescent imaging), and confirmation was made that treatment groups had equivalent average luminescence at time of treatment.

Mice litters from each experimental group were randomized to treatment with: (A) 25 mg/kg dasatinib or 10 mg/Kg everolimus alone (10% dasatinib or everolimus suspended in DMSO, 80% ultra-pure water, 10% Tween-80), (B) control treatment (10% DMSO, 80% ultra-pure water, 10% Tween-80), (C) a “low-dose” combination group which received 10 mg/kg dasatinib and 5 mg/kg everolimus (10% dasatinib or everolimus suspended in DMSO, 80% ultra-pure water, 10%, Tween-80), and (D) a

"high-dose" combination group which received 25 mg/kg dasatinib and 10 mg/kg everolimus (10% dasatinib or everolimus suspended in DMSO, 80% ultra-pure water, 10%, Tween-80). Initial studies with the high-dose combination were associated with early treatment-related morbidity/mortality; therefore, this arm was excluded from further studies.

Animals displaying symptoms of morbidity after treatment were euthanized for immunohistochemical or pharmacodynamic/ pharmacokinetic (PD/PK) tumor. For immunohistochemistry analysis, mice were perfused with Tyrode's Solution followed by 4% paraformaldehyde fixative solution to preserve the structures of the brain.

Human PDGFRA-driven glioma treatment, CSF PK and cerebrospinal tumor DNA (CSF-tDNA) collection.

Pharmacokinetic analysis

Mouse PK sample procurement

Drug administration to non-tumor bearing C57/Bl6 mice for PK studies were performed by oral gavage administration of everolimus two hours prior to a tail vein injection of dasatinib. At one, two, four and seven hours after the dasatinib injection, the mice were isoflurane/oxygen-anesthetized and 500 uL to 1 mL of blood was drawn from the apex of the heart within the mouse's enclosed cavity. Immediately, the withdrawn blood was centrifuged within a microvette EDTA coated conical tube for 10 minutes at 10,000 RPM, and the plasma was separated and stored at -80°C until PK analysis was performed. Following the blood draw, the mouse was sacrificed and the brain, brain stem, and/or tumor were extracted separately and stored at -80°C until PK analysis was performed.

Chemicals and reagents

For PK studies, dasatinib powder was procured from Sigma-Aldrich. Liquid chromatography–mass spectrometry (LC-MS) grade acetonitrile was purchased from Sigma-Aldrich. Formic acid (98%; LC-MS grade) was obtained from Fluka. A Milli-Q water system from Millipore was used to obtain ultrapure deionized water.

Stock solutions, working solutions, and quality control samples

Dasatinib and the internal standard were individually weighed and dissolved in acetonitrile to stock solutions and then stored at −20°C. The dasatinib stock solution was then diluted with acetonitrile to a series of working solutions from 2.5 to 5,000 ng/mL The quality control working solutions at low, medium, and high concentrations were prepared using a separately prepared stock solution. For sample preparation, the dasatinib stock solution was diluted to 1,000 ng/mL with acetonitrile. Quality control samples were evenly distributed among samples from each batch.

Sample preparation

Plasma (40 µL) was dispensed into a Fisher Scientific 96-well plate, to which 40 µL of ice-cold acetonitrile (100%) and 120 µL of internal standard solution (1000 ng/mL) were added. Next, the plate was vortexed for 10 minutes. The plate was then centrifuged at 3500 revolutions per minute (RPM) for 10 minutes at 4°C to precipitate the protein. LC–tandem mass spectrometry (LC-MS/MS) was used to analyze 5 µL of the supernatant. The plasma samples were sonicated prior to being transferred to the 96-well plates. Tissue samples were weighed and suspended in 20% acetonitrile (80% water; 1:5 wt/vol). The samples were then homogenized four times for 20 seconds each time at 6,500 RPM in a Precellys Evolution system. For LC-MS/MS analysis, the dasatinib in brain tissue homogenates were extracted from the samples in the same

manner as the dasatinib in plasma. Prior to extraction, samples that were above the upper limit of qualification were diluted with the same matrix. Calibrator-standard samples and quality control samples were prepared by mixing 40 µL of blank bio matrix, 40 µL of working solution, and 120 µL of internal standard solution.

Calibration curve

Analytical curves were made with 12 nonzero standards by plotting the peak area ratio of dasatinib to the internal standard vs the concentration. The curve was created with linear regression and weighted (1/X2). The correlation coefficient demonstrated the linearity of the relationship between peak area ratio and concentration.

Liquid chromatography tandem–mass spectrometry

The concentrations of dasatinib were determined with a Sciex AB-5500 Qtrap mass spectrometer with electrospray ionization source, interfaced with a Shimadzu high-performance LC system. The LC-MS/MS system was controlled with Analyst Software version 1.6 from Applied Biosystems; this was also used for acquisition and processing of data. Separation was performed on a Waters Xbridge C18 column (50 × 2.1 mm ID, 3.5 µm); the flow rate was 0.4 mL/min. A (100% H2O with 0.1% formic acid) and B (100% acetonitrile with 0.1% formic acid) comprised the mobile phase. The gradient began with 5% B for 30 seconds and then linearly increased to 99% B at 2 minute and then reduced to 5% B at 4.1 minutes to 5.5 minutes with a runtime of 6 minutes in total. The mass spectrometer was operated in positive mode; multiple reaction monitoring was used for analysis. The Q1 m/z and Q3 m/z was 487.9 and 401.1, respectively.

Approval of the Human Study

Two patients were treated with dasatinib and everolimus for children and adults with newly diagnosed (post-radiation) high-grade (grade III-IV) glioma or recurrent grade II-IV glioma with *PDGF* alterations. This institutional protocol was approved by the University of Michigan Institutional Review Board and registered on clinicaltrials.gov (NCT03352427). Patients or their legal guardian provided informed consent for treatment on this protocol. Enrollment required CLIA-certified confirmation of a DNA (mutation, amplification) or RNA (fusion) alteration in a PDGF-related gene (*PDGFRA*, *PDGFA*, *PDGFRB*, *PDGFB*). Paired CSF/plasma samples (before and after addition of everolimus) were collected from enrolled patients.

Patients received dasatinib 60 mg/m2 orally twice daily and everolimus 3 mg/m2 orally once daily continuously, with titration of dosing to maintain an everolimus trough level of 5-15 ng/mL. Cycles were repeated every 28 days for up to 24 cycles. CSF and serum dasatinib pharmacokinetics were performed by the University of Michigan Pharmacokinetic Core Facility (see supplemental methods) to determine whether blood-CSF permeability of dasatinib is impacted by dual therapy with everolimus. Prior to the first cycle, dasatinib was taken as mono-therapy for one week followed by CSF collection in order to establish a mono-therapy dasatinib CSF level. After the second cycle, CSF was collected to establish a dual-therapy dasatinib level (while on everolimus). Additionally, all CSF samples were assessed for cell-free tumor DNA (cf-tDNA) using previous methods (32), when sample remained.

Human HGG clinical sequencing and PDGFRA *alteration confirmation*

For confirmation of *PDGFRA* status in human HGG patients, tumor (FFPE or frozen) and normal (cheek swab) samples were submitted for whole exome (paired tumor and germline DNA) and transcriptome (tumor RNA) sequencing. Clinically-integrated sequencing was performed according to previously published methodology (33,34). Nucleic acid preparation, high-throughput sequencing, and computational analysis were performed by the Michigan Center for Translational Pathology (MCTP) sequencing laboratory using standard protocols in adherence to the Clinical Laboratory Improvement Amendments (CLIA).

Human P-gp expression

Pediatric and adult human P-gp expression dataset analysis was performed using RNA-seq data accessed from PedcBioPortal. For pediatric HGG, data was accessed from the Pediatric HGG ICR London (2). We performed comparisons of P-gp expression by location of tumor, H3 (*H3F3A* or *HIST1H3B*) mutation status, *PDGFRA* mutation status, and age. For adult HGG, data was accessed from The Cancer Genome Atlas dataset (24) (24). For TCGA (adult HGG) P-gp RNA, we compared P-gp expression levels by *PDGFRA* mutation status, age and methylguanine-DNA methyltransferase (MGMT) status.

Statistics

For comparison of dose-response curves using DNA-damaging agents, a nonlinear regression curve [log (agent) vs. normalized response with variable slope]

was generated. Statistical significance in all experiments was defined as a two-sided $P \leq 0.05$. All analyses were conducted with GraphPad Prism software (version 7.00). Expression level of P-gp, PDGFRA and p-AKT were quantified using IHC performed on mouse brain section treated with everolimus and/or dasatinib. Five to six randomly selected JPEG images were captured from each IHC slide at 40x magnification on the Aperio image scope and quantified using ImageJ software. ImageJ software was also used to quantify PPK neurosphere area in squared pixel unit, with comparisons between treatment groups using Welch's t-test.

AUTHOR CONTRIBUTIONS: *In vitro* experimental design, experiments and data analysis: Z.M., B.M., V.Y., C.K.; *In vivo* experimental design, experiments and data analysis : Z.M., V.Y., B.M. T.G., T.P., T.Y.; Clinical/human correlate research: Z.M., R.S., B.M., K.W., A.B., S.S., H.G., A.P., I.W., M.L., P.R., C.K.-S., A.C., R.M., C.K.; Pharmacokinetic analysis: Z.M., M.P., B.M. C.K; Manuscript preparation: Z.M., B.M., C.K, V.Y., R.S., R.C., S.V.; All authors discussed and reviewed the manuscript and approved the manuscript for publication.

ACKNOWLEDGMENTS: The authors thank the patients and their families for participation in this study.

REFERENCES:

1. Liu J, Lichtenberg T, Hoadley KA, et al. An Integrated TCGA Pan-Cancer Clinical Data Resource to Drive High-Quality Survival Outcome Analytics. *Cell.* 2018;173(2):400-416 e411.
2. Mackay A, Burford A, Carvalho D, et al. Integrated Molecular Meta-Analysis of 1,000 Pediatric High-Grade and Diffuse Intrinsic Pontine Glioma. *Cancer Cell.* 2017;32(4):520-537 e525.
3. Farahani RM, Xaymardan M. Platelet-Derived Growth Factor Receptor Alpha as a Marker of Mesenchymal Stem Cells in Development and Stem Cell Biology. *Stem Cells Int.* 2015;2015:362753.
4. Mackay A, Burford A, Molinari V, et al. Molecular, Pathological, Radiological, and Immune Profiling of Non-brainstem Pediatric High-Grade Glioma from the HERBY Phase II Randomized Trial. *Cancer Cell.* 2018;33(5):829-842 e825.
5. Koschmann C, Zamler D, MacKay A, et al. Characterizing and targeting PDGFRA alterations in pediatric high-grade glioma. *Oncotarget.* 2016;7(40):65696-65706.
6. Alentorn A, Marie Y, Carpentier C, et al. Prevalence, clinico-pathological value, and co-occurrence of PDGFRA abnormalities in diffuse gliomas. *Neuro Oncol.* 2012;14(11):1393-1403.
7. Paugh BS, Zhu X, Qu C, et al. Novel oncogenic PDGFRA mutations in pediatric high-grade gliomas. *Cancer Res.* 2013;73(20):6219-6229.
8. Lassman AB, Pugh SL, Gilbert MR, et al. Phase 2 trial of dasatinib in target-selected patients with recurrent glioblastoma (RTOG 0627). *Neuro Oncol.* 2015;17(7):992-998.

9. Motzer RJ, Hutson TE, Glen H, et al. Lenvatinib, everolimus, and the combination in patients with metastatic renal cell carcinoma: a randomised, phase 2, open-label, multicentre trial. *The lancet oncology.* 2015;16(15):1473-1482.

10. Pignochino Y, Dell'Aglio C, Basiricò M, et al. The Combination of Sorafenib and Everolimus Abrogates mTORC1 and mTORC2 upregulation in osteosarcoma preclinical models. *Clinical Cancer Research.* 2013;19(8):2117-2131.

11. Porkka K, Koskenvesa P, Lundan T, et al. Dasatinib crosses the blood-brain barrier and is an efficient therapy for central nervous system Philadelphia chromosome-positive leukemia. *Blood.* 2008;112(4):1005-1012.

12. Agarwal S, Mittapalli RK, Zellmer DM, et al. Active efflux of Dasatinib from the brain limits efficacy against murine glioblastoma: broad implications for the clinical use of molecularly targeted agents. *Molecular cancer therapeutics.* 2012;11(10):2183-2192.

13. Minocha M, Khurana V, Qin B, Pal D, Mitra AK. Enhanced brain accumulation of pazopanib by modulating P-gp and Bcrp1 mediated efflux with canertinib or erlotinib. *Int J Pharm.* 2012;436(1-2):127-134.

14. Oberoi RK, Mittapalli RK, Elmquist WF. Pharmacokinetic assessment of efflux transport in sunitinib distribution to the brain. *J Pharmacol Exp Ther.* 2013;347(3):755-764.

15. Benes C, Haber DA, Beare D, et al. Genomics of Drug Sensitivity in Cancer (GDSC): a resource for therapeutic biomarker discovery in cancer cells. *Nucleic Acids Research.* 2012;41(D1):D955-D961.

16. Mittapalli RK, Chung AH, Parrish KE, et al. ABCG2 and ABCB1 limit the efficacy of dasatinib in a PDGF-B–Driven brainstem glioma model. *Molecular cancer therapeutics.* 2016;15(5):819-829.

17. de Vries NA, Zhao J, Kroon E, Buckle T, Beijnen JH, van Tellingen O. P-glycoprotein and breast cancer resistance protein: two dominant transporters working together in limiting the brain penetration of topotecan. *Clinical Cancer Research.* 2007;13(21):6440-6449.

18. Dash RP, Babu RJ, Srinivas NR. Therapeutic potential and utility of elacridar with respect to P-glycoprotein inhibition: An insight from the published in vitro, preclinical and clinical studies. *European journal of drug metabolism and pharmacokinetics.* 2017;42(6):915-933.

19. Lagas JS, van Waterschoot RA, van Tilburg VA, et al. Brain accumulation of dasatinib is restricted by P-glycoprotein (ABCB1) and breast cancer resistance protein (ABCG2) and can be enhanced by elacridar treatment. *Clinical Cancer Research.* 2009;15(7):2344-2351.

20. Minocha M, Khurana V, Qin B, Pal D, Mitra AK. Co-administration strategy to enhance brain accumulation of vandetanib by modulating P-glycoprotein (P-gp/Abcb1) and breast cancer resistance protein (Bcrp1/Abcg2) mediated efflux with m-TOR inhibitors. *International journal of pharmaceutics.* 2012;434(1-2):306-314.

21. Warren KE. Beyond the Blood:Brain Barrier: The Importance of Central Nervous System (CNS) Pharmacokinetics for the Treatment of CNS Tumors, Including Diffuse Intrinsic Pontine Glioma. *Front Oncol.* 2018;8:239.

22. Ruggiero A, Cefalo G, Garre ML, et al. Phase II trial of temozolomide in children with recurrent high-grade glioma. *J Neurooncol.* 2006;77(1):89-94.

23. Narayana A, Kunnakkat S, Chacko-Mathew J, et al. Bevacizumab in recurrent high-grade pediatric gliomas. *Neuro Oncol.* 2010;12(9):985-990.

24. Brennan CW, Verhaak RG, McKenna A, et al. The somatic genomic landscape of glioblastoma. *Cell.* 2013;155(2):462-477.

25. Minocha M, Khurana V, Qin B, Pal D, Mitra AK. Co-administration strategy to enhance brain accumulation of vandetanib by modulating P-glycoprotein (P-gp/Abcb1) and breast cancer resistance protein (Bcrp1/Abcg2) mediated efflux with m-TOR inhibitors. *Int J Pharm.* 2012;434(1-2):306-314.

26. Wolburg H, Noell S, Fallier-Becker P, Mack AF, Wolburg-Buchholz K. The disturbed blood-brain barrier in human glioblastoma. *Mol Aspects Med.* 2012;33(5-6):579-589.

27. Kalvass JC, Polli JW, Bourdet DL, et al. Why clinical modulation of efflux transport at the human blood-brain barrier is unlikely: the ITC evidence-based position. *Clin Pharmacol Ther.* 2013;94(1):80-94.

28. O'Donnell A, Faivre S, Burris III HA, et al. Phase I pharmacokinetic and pharmacodynamic study of the oral mammalian target of rapamycin inhibitor everolimus in patients with advanced solid tumors. *Journal of Clinical Oncology.* 2008;26(10):1588-1595.

29. Dewaele B, Wasag B, Cools J, et al. Activity of dasatinib, a dual SRC/ABL kinase inhibitor, and IPI-504, a heat shock protein 90 inhibitor, against gastrointestinal stromal tumor-associated PDGFRAD842V mutation. *Clin Cancer Res.* 2008;14(18):5749-5758.

30. Nitarska J, Smith JG, Sherlock WT, et al. A Functional Switch of NuRD Chromatin Remodeling Complex Subunits Regulates Mouse Cortical Development. *Cell Rep.* 2016;17(6):1683-1698.

31. Chou TC. Drug combination studies and their synergy quantification using the Chou-Talalay method. *Cancer Res.* 2010;70(2):440-446.

32. Stallard S, Savelieff MG, Wierzbicki K, et al. CSF H3F3A K27M circulating tumor DNA copy number quantifies tumor growth and in vitro treatment response. *Acta neuropathologica communications.* 2018;6(1):80.

33. Miklja Z, Pasternak A, Stallard S, et al. Molecular profiling and targeted therapy in pediatric gliomas: review and consensus recommendations. *Neuro Oncol.* 2019.

34. Koschmann C, Wu Y-M, Kumar-Sinha C, et al. Clinically Integrated Sequencing Alters Therapy in Children and Young Adults With High-Risk Glial Brain Tumors. *JCO Precision Oncology.* 2018(2):1-34.

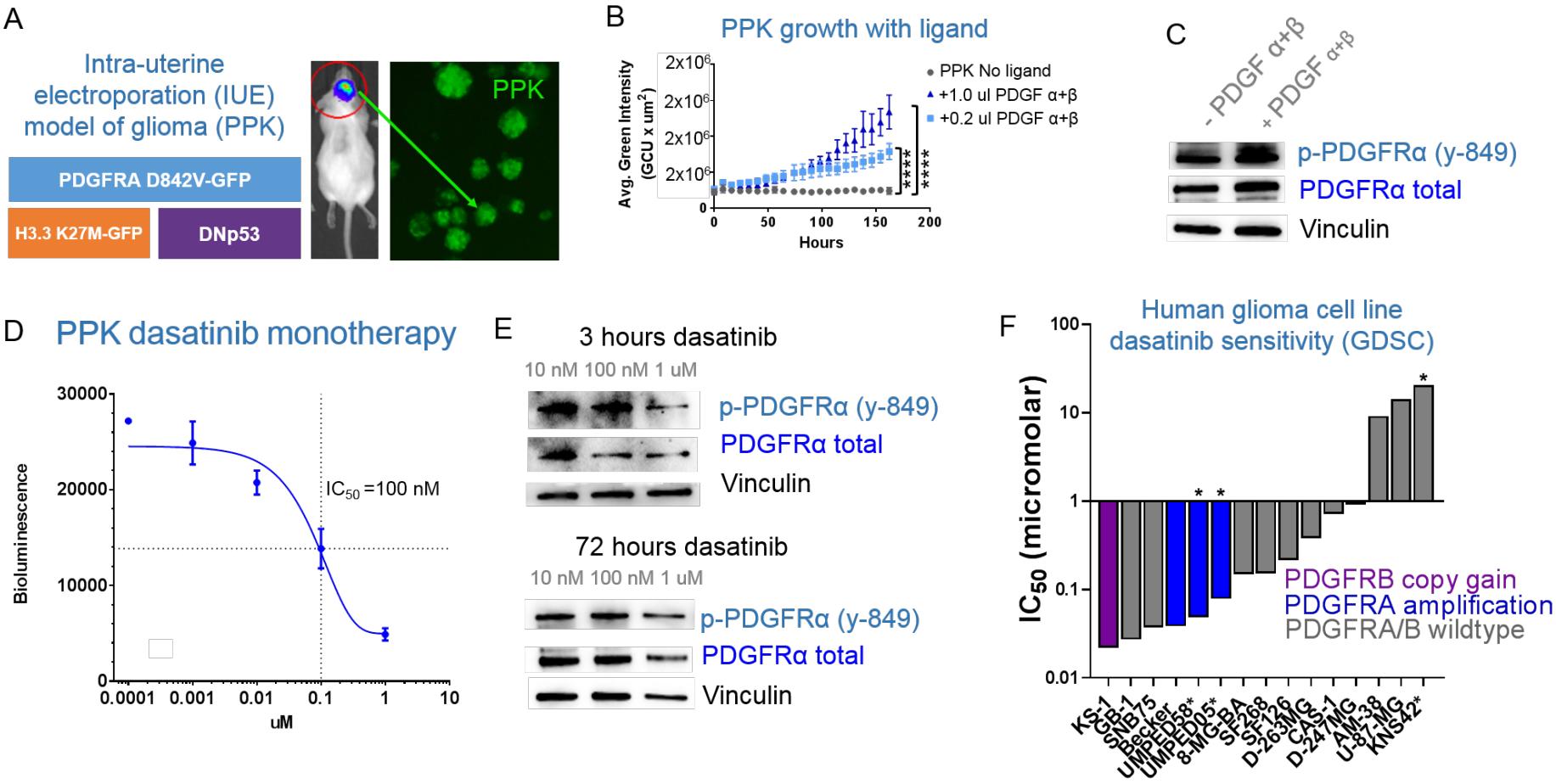

Figure 1: PDGRA-driven glioma demonstrates sensitivity to dasatinib *in vitro* **A)** HGG cells are generated from an intra-uterine electroporation (IUE) model with plasmids of *TP53*, *PDGFRA* and H3K27M mutations. **B)** Proliferation of IUE HGG cells in response to adding PDGF ligand α and β *in vitro* (**** $P \leq 0.00005$ by Welch's t-test). **C)** Western blot analysis of p-PDGFRA and total PDGFRA total in response to PDGF ligand addition. **D)** Dose response curve of PPK neurospheres to treatmeant with dasatinib. **E)** Western blot analysis documenting dasatinib monotherapy of p-PDGFRA and total PDGFRA after 3 hours and 72 hours of dasatinib monotherapy. **F)** Plot of glioma cell culture sensitivity to dasatinib from Genomics of Drug Sensitivity in Cancer (GDSC). Analysis of *PDGFRA, PDGFRB, PDGFRA and PDGFRB* DNA-alterations is referenced (*non-GDSC data generated from primary cell culture treatment for this study).

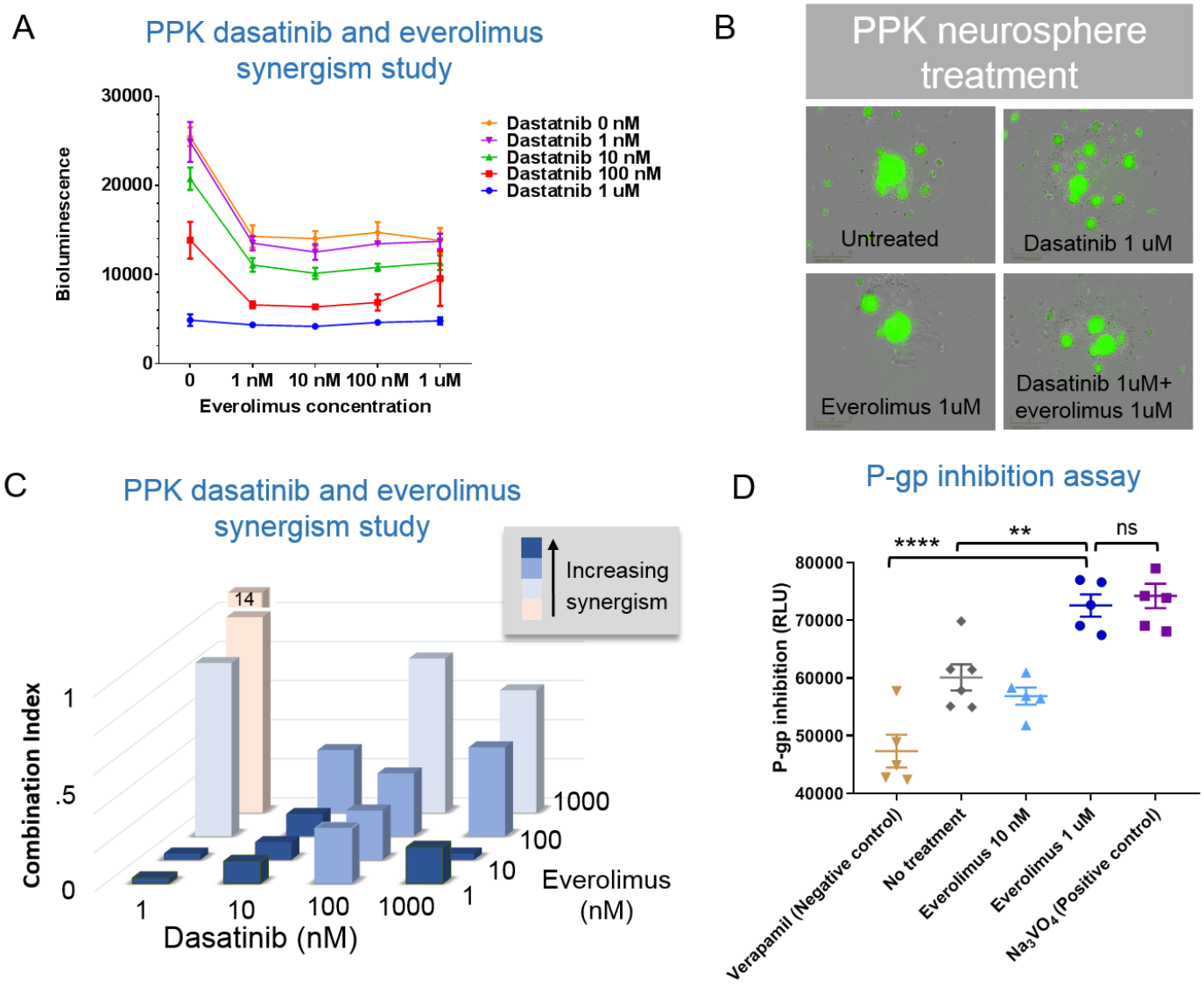

Figure 2: Addition of everolimus provides synergism and strong p-glycoprotein (P-gp) blockade **A)** Viability of IUE HGG neurosphere in response to various combinations of dasatinib and everolimus. **B)** Microscopic images of IUE PPK neurospheres after 72 hours of treatment with four separate conditions. **C)** Everolimus and dasatinib synergism combination index. **D)** Plot of P-gp inhibition using *in vitro* assay with controls (higher numbers = greater P-gp inhibition).

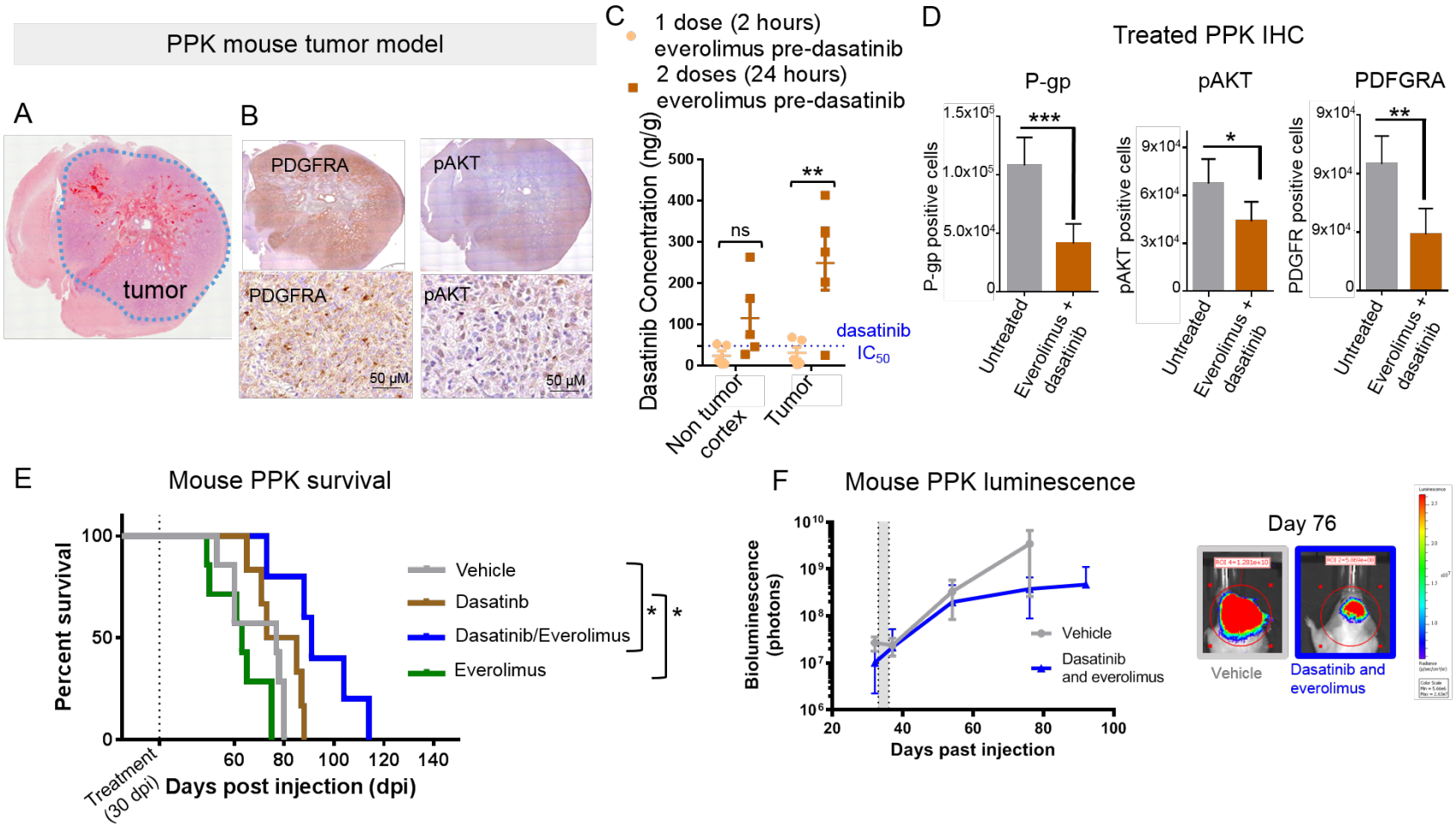

Figure 3: Sustained exposure of everolimus improves dasatinib tumor concentration and efficacy in mouse model **A)** Representative cortical plane of mouse brain with PPK tumor (80-90% cortex effaced). **B)** p-AKT and PDGFRA positive immunohistochemistry staining in IUE HGG tumor *in vivo*. **C)** Pharmacokinetic data documenting increase in dasatinib levels found in tumors with additional 24 hour everolimus pre-dasatinib dose (** $P \leq 0.01$ by Welch's t-test). **D)** *In vivo* immunohistochemistry of P-gp, pAKT and PDFGR expression level documenting a reduction with everolimus and dasatinib treatment in comparison to non-treated tumors (*** $P \leq 0.0005$, * $P \leq 0.05$, ** $P \leq 0.005$ by Welch's t-test, respectfully). **E)** IUE PDGFRA survival curve data demonstrates that median survival for the control condition was 77 days post IUE injection; the everolimus (10mg/kg) condition was 63 days; the dasatinib (25mg/kg) was 79 days; and the dasatinib and everolimus condition (10 mg/kg and 5mg/kg, respectively) was 91 days. **F)** IUE PDGFRA bioluminescence tumor monitor growth data and representative images of mice tumors at day 76. Scale bars: B (50 μm).

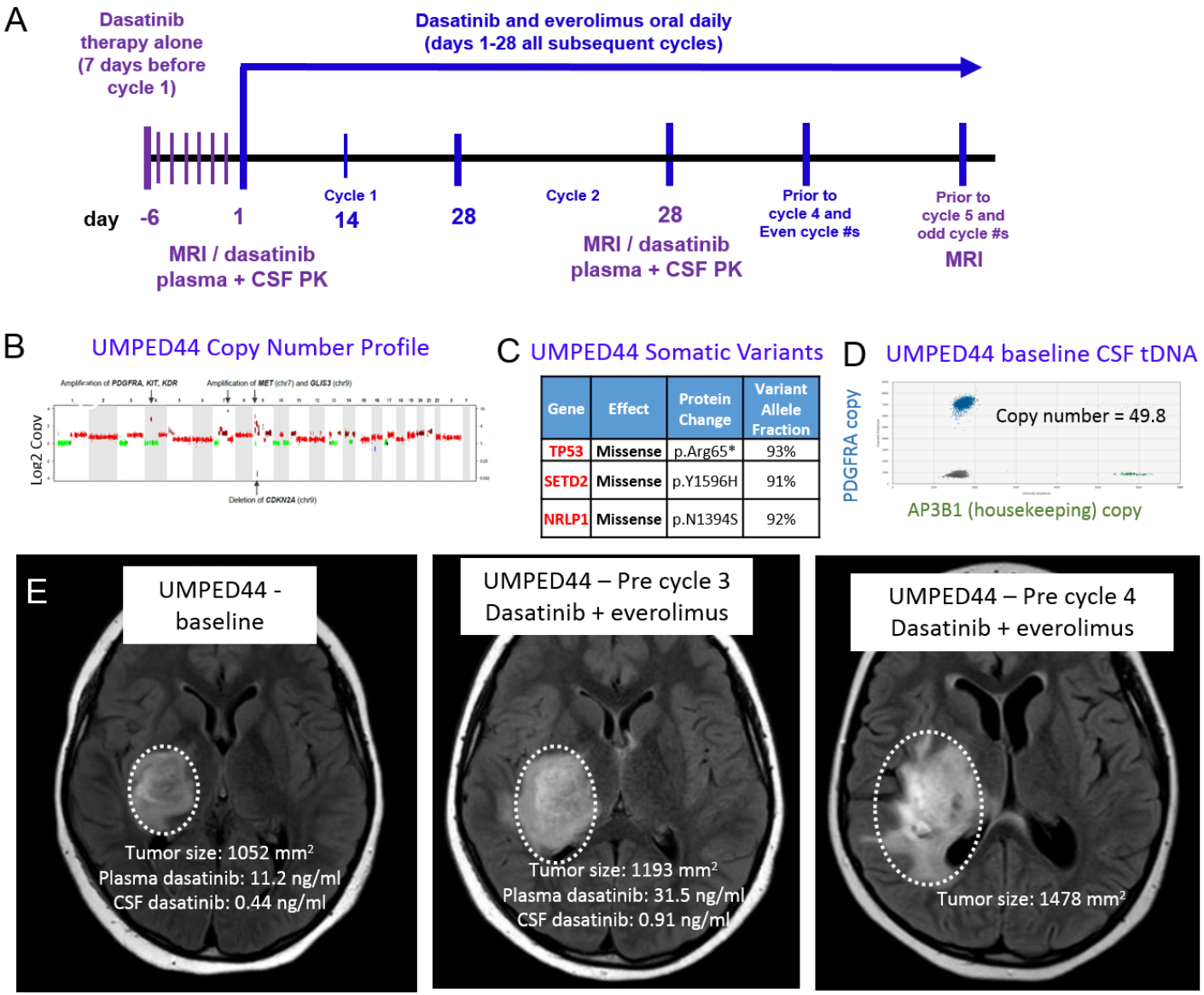

Gene	Effect	Protein Change	Variant Allele Fraction
TP53	Missense	p.Arg65*	93%
SETD2	Missense	p.Y1596H	91%
NRLP1	Missense	p.N1394S	92%

Figure 4: Treatment of UMPED44 with relapsed *PDGFRA*-amplified HGG A) Schematic depicting phase-2 clinical trial design for patients. UMPED44 B) copy number profile, C) somatic alterations, and D) baseline CSF tDNA copy number (49.8). E) UMPED44 axial FLAIR MRI at baseline, pre cycle 3, and pre cycle 4.

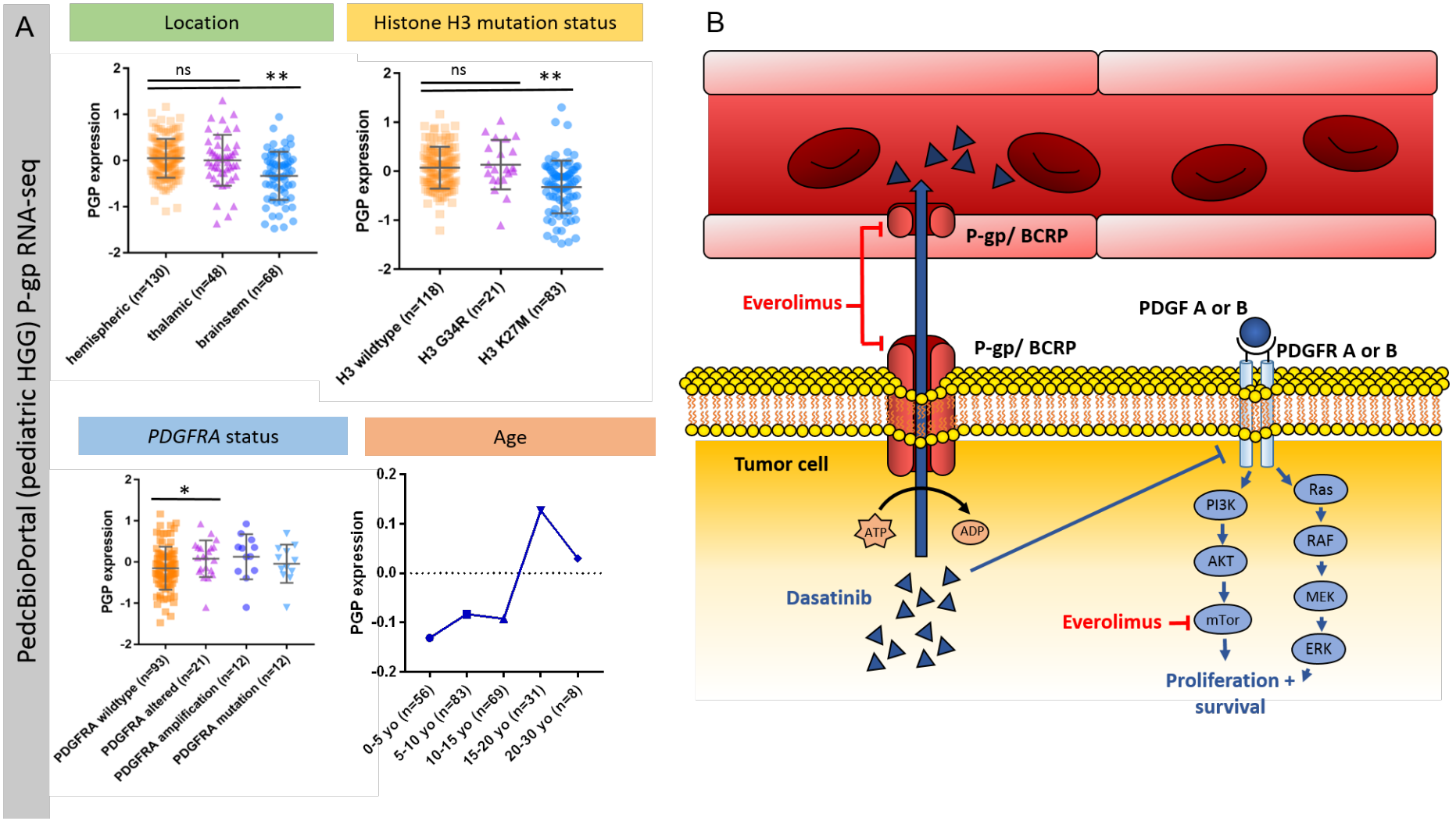

Figure 5: P-gp expression in human pediatric HGG and proposed schema. **A)** PedcBioPortal (pediatric HGG) P-gp RNA-seq data by location. **B)** Schematic representation of dasatinib and everolimus targeting of PDGF-driven HGG.